Supplemental material to this article can be found at:
http://dmd.aspetjournals.org/content/suppl/2013/07/02/dmd.113.052084.DC1.html

1521-009X/41/9/1703–1714$25.00
Drug Metabolism and Disposition
http://dx.doi.org/10.1124/dmd.113.052084
Drug Metab Dispos 41:1703–1714, September 2013
Copyright © 2013 by The American Society for Pharmacology and Experimental Therapeutics

Biotransformation of a Novel Positive Allosteric Modulator of Metabotropic Glutamate Receptor Subtype 5 Contributes to Seizure-Like Adverse Events in Rats Involving a Receptor Agonism-Dependent Mechanism[S]

Thomas M. Bridges, Jerri M. Rook, Meredith J. Noetzel, Ryan D. Morrison, Ya Zhou, Rocco D. Gogliotti, Paige N. Vinson, Zixiu Xiang, Carrie K. Jones, Colleen M. Niswender, Craig W. Lindsley, Shaun R. Stauffer, P. Jeffrey Conn, and J. Scott Daniels

Departments of Pharmacology (T.M.B., R.D.M., Y.Z., R.D.G., J.S.D., J.M.R., M.J.N., P.N.V., Z.X., C.M.N., P.J.C., C.K.J., C.W.L., S.R.S.) and Chemistry (C.W.L.),Vanderbilt Center for Neuroscience Drug Discovery, Vanderbilt University Medical Center, Nashville, Tennessee

Received March 21, 2013; accepted July 2, 2013

ABSTRACT

Activation of metabotropic glutamate receptor subtype 5 ($mGlu_5$) represents a novel strategy for therapeutic intervention into multiple central nervous system disorders, including schizophrenia. Recently, a number of positive allosteric modulators (PAMs) of $mGlu_5$ were discovered to exhibit in vivo efficacy in rodent models of psychosis, including PAMs possessing varying degrees of agonist activity (ago-PAMs), as well as PAMs devoid of agonist activity. However, previous studies revealed that ago-PAMs can induce seizure activity and behavioral convulsions, whereas pure $mGlu_5$ PAMs do not induce these adverse effects. We recently identified a potent and selective $mGlu_5$ PAM, VU0403602, that was efficacious in reversing amphetamine-induced hyperlocomotion in rats. The compound also induced time-dependent seizure activity that was blocked by coadministration of the $mGlu_5$ antagonist, 2-methyl-6-(phenylethynyl) pyridine. Consistent with potential adverse effects induced by ago-PAMs, we found that VU0403602 had significant allosteric agonist activity. Interestingly, inhibition of VU0403602 metabolism in vivo by a pan cytochrome P450 (P450) inactivator completely protected rats from induction of seizures. P450-mediated biotransformation of VU0403602 was discovered to produce another potent ago-PAM metabolite-ligand (M1) of $mGlu_5$. Electrophysiological studies in rat hippocampal slices confirmed agonist activity of both M1 and VU0403602 and revealed that M1 can induce epileptiform activity in a manner consistent with its proconvulsant behavioral effects. Furthermore, unbound brain exposure of M1 was similar to that of the parent compound, VU0403602. These findings indicate that biotransformation of $mGlu_5$ PAMs to active metabolite-ligands may contribute to the epileptogenesis observed after in vivo administration of this class of allosteric receptor modulators.

Introduction

Initiated largely by the *N*-methyl-D-aspartate receptor hypofunction hypothesis, we and others have identified metabotropic glutamate receptor subtype 5 ($mGlu_5$) as a potential means for therapeutic intervention in central nervous system (CNS) disorders such as schizophrenia (Olney et al., 1999; Tsai and Coyle, 2002; Conn et al., 2009; Marek et al., 2010; Gregory et al., 2011; Vinson and Conn, 2012). To this end, we have successfully identified potent and selective positive allosteric modulators (PAMs) of $mGlu_5$ that are orally active in rodent models of psychosis and in various cognitive paradigms (Hammond et al., 2010; Rodriguez et al., 2010; Williams et al., 2011). Recently, we described several PAMs possessing intrinsic agonist activity that stimulate glutamate-independent signaling (Noetzel et al., 2012). Some of these agonist-PAM (ago-PAM) compounds induce $mGlu_5$-dependent limbic seizures similar to the adverse events (AEs) reported in rodents receiving intracerebral administration of the $mGlu_5$ agonist, dihydroxyphenylglycine (DHPG) (Tizzano et al., 1995a,b; Rook et al., 2012). Moreover, results from electrophysiological experiments confirm an

This work was supported by the National Institutes of Health [Grants R01-MH062646, R01-MH074953, and U01-MH087965].

Portions of this work were previously presented: Bridges T, Morrison R, Daniels J (2012) *North American Meetings of the International Society for the Study of Xenobiotics*, October 2012, Dallas, TX.

dx.doi.org/10.1124/dmd.113.052084.

[S]This article has supplemental material available at dmd.aspetjournals.org.

ABBREVIATIONS: 1-ABT, 1-aminobenzotriazole; ACSF, artificial cerebrospinal fluid; AE, adverse event; ago-PAM, positive allosteric modulator with agonist activity; AUC, area under the curve; CL_{int}, intrinsic clearance; CNS, central nervous system; CRC, concentration-response curve; DHPG, dihydroxyphenylglycine; DME, drug-metabolizing enzyme; DMEM, Dulbecco's modified Eagle's medium; DMPK, drug metabolism and pharmacokinetics; DMSO, dimethylsulfoxide; FBS, fetal bovine serum; fEPSP, field excitatory postsynaptic potential; GIRK, G-protein–coupled inwardly rectifying potassium channel; HEK293A, human embryonic kidney cell line 293A; HPLC, high-performance liquid chromatography; 5-HT, human serotonin; LTD, long-term depression; $mGlu_5$, metabotropic glutamate receptor subtype 5; MPEP, 2-methyl-6-(phenylethynyl) pyridine; NAM, negative allosteric modulation; P450, cytochrome P450; PAM, positive allosteric modulator; PO, by mouth; RCF, relative centrifugal force; RED, rapid equilibrium dialysis; S9, subcellular fraction containing microsomes and cytosol; SAM, silent allosteric modulation; SAR, structure-activity relationship; TFA, trifluoroacetic acid.

Downloaded from dmd.aspetjournals.org at ASPET Journals on March 14, 2015

induction of epileptiform activity after treatment of rat hippocampal slices with $mGlu_5$ agonists; this effect was attenuated by an $mGlu_5$ antagonist (Lee et al., 2002; Zhao et al., 2004; Wong et al., 2005). Collectively, our observations are consistent with recent assertions that group I $mGlu_5$ activation can be a critical initiation step contributing to propagation of epileptogenic discharges in the CNS (Wong et al., 2005).

We previously reported on a group of highly selective $mGlu_5$ allosteric modulators displaying favorable pharmacokinetic properties and PAM or ago-PAM activity as determined by Ca^{2+} mobilization in recombinant cells and in cortical astrocytes (Rook et al., 2012) (Fig. 1). Importantly, electrophysiological experiments indicated that ago-PAMs such as VU0424465 induced prolonged long-term depression (LTD) and increased both the amplitude and frequency of spontaneous population spikes determined by extracellular field potential recordings in rat hippocampal slices (Rook et al., 2012). However, PAMs that were devoid of intrinsic agonist activity (VU0360172 and VU0361747) did not induce epileptiform activity (Rook et al., 2012). Finally, rats receiving a systemic administration of the ago-PAM, VU0424465, experienced pronounced seizures, which were completely prevented by pretreatment with the selective $mGlu_5$ antagonist, 2-methyl-6-(phenylethynyl) pyridine (MPEP) (Rook et al., 2012).

We have observed that several $mGlu_5$ PAM chemical series contain compounds possessing diverse modes of pharmacology, including positive allosteric modulation, negative allosteric modulation (NAM), and silent allosteric modulation (SAM) (Sharma et al., 2009; Lamb et al., 2011; Lindsley, 2011; Williams et al., 2011; Wood et al., 2011). In many cases, single-atom modifications to compounds have resulted in a molecular switch that effectively converts PAMs to NAMs or ago-PAMs. This propensity for pharmacological "mode-switching" represents a barrier to the optimization of $mGlu_5$ allosteric modulators owing to the range of drug-metabolizing enzymes (DMEs) that are capable of introducing subtle single atom oxidations to PAMs. Biotransformation of a PAM could result in the formation of active metabolites capable of 1) silencing the effect (i.e., SAM) of the parent compound, 2) activating the receptor in the absence of glutamate (ago-PAMs), or 3) reversing the allosteric modulation (i.e., NAM) of the parent PAM in vivo.

Herein, we describe the in vitro and in vivo pharmacology and drug metabolism and pharmacokinetic (DMPK) profile of a selective $mGlu_5$ ago-PAM, VU0403602, which induced pronounced dose- and time-dependent seizures in rats, an effect that was prevented by pretreatment with MPEP. Together, these data indicate an $mGlu_5$-mediated mechanism to the neurotoxicity observed in vivo. Interestingly, pretreatment of rats with the pan cytochrome P450 (P450) inactivator 1-aminobenzotriazole (ABT) effectively prevented VU0403602-induced seizures, further implicating the role of a metabolite-ligand in the onset of AEs. In vivo pharmacokinetic studies revealed that both parent VU0403602 and the metabolite permeated the CNS of rats and that the exposure of the metabolite was significantly reduced in rats that had been pretreated with ABT. An in vitro and in vivo appraisal of the metabolism of VU0403602 identified a principal oxidative metabolite that displayed potent ago-PAM activity. Additional studies involving systemic administration of the metabolite to rats resulted in a rapid onset of seizures, the severity of which was similar to that observed after the administration of VU0403602. Subsequent in vitro electrophysiological experiments indicated that the metabolite-ligand induced prolonged LTD and epileptogenic discharges in rat hippocampal slices, similar to those observed with the $mGlu_5$ agonist DHPG (Tizzano et al., 1995a,b; Lee et al., 2002; Zhao et al., 2004; Wong et al., 2005). Together, these findings support the hypothesis that the $mGlu_5$ ago-PAM VU0403602 undergoes P450-mediated biotransformation to an active metabolite, which itself possesses potent agonist-PAM activity and subsequently contributes to proconvulsant behavioral effects in vivo.

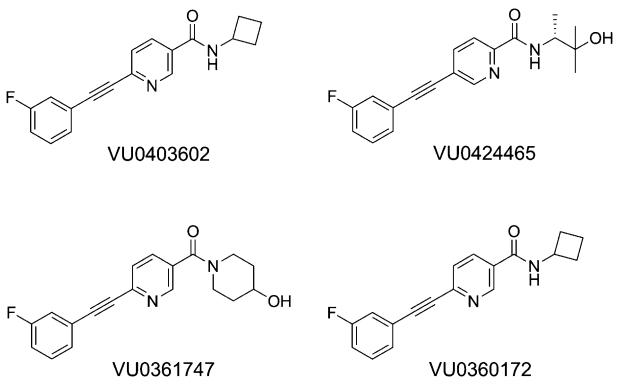

Fig. 1. Structures of $mGlu_5$ allosteric modulators.

Materials and Methods

Reagents

VU0403602 (*N*-cyclobutyl-5-((3-fluorophenyl)ethynyl)picolinamide) and metabolites M1 and M2 (5-((3-fluorophenyl)ethynyl)-*N*-(3-hydroxycyclobutyl) picolinamide and 5-((3-fluorophenyl)ethynyl)picolinic acid, respectively) were prepared by the Medicinal Chemistry Laboratories of the Vanderbilt Center for Neuroscience Drug Discovery. Potassium phosphate, ammonium formate, formic acid, NADPH, magnesium chloride ($MgCl_2$), adenosine 3′-phosphate 5′-phosphosulfate lithium salt hydrate, uridine 5′-diphosphoglucuronic acid trisodium salt, and 1-aminobenzotriazole (ABT) were purchased from Sigma-Aldrich Chemical Company (St. Louis, MO). Rat hepatic subcellular fractions were obtained from BD Biosciences (Woburn, MA). Rat brain S9 fractions were obtained from Celsis In Vitro Technologies (Baltimore, MD). Rat intestinal S9 fractions were obtained from Xenotech (Lenexa, KS). Dulbecco's modified Eagle's medium (DMEM), fetal bovine serum (FBS), and antibiotics were purchased from Invitrogen (Carlsbad, CA). DHPG was obtained from Ascent Scientific (Bristol, UK). [^{3}H]mPEPy was purchased from PerkinElmer (Waltham, MA). 5MPEP and MPEP were synthesized as described previously.

Chemical Synthesis

General. All NMR spectra were recorded on a Bruker 400-mHz instrument (Bruker, Billerica, MA). ^{1}H chemical shifts are reported in δ values in parts per million downfield from TMS (tetramethylsilane) as the internal standard in d_3-MeOH. Data are reported as follows: chemical shift, multiplicity (s = singlet, d = doublet, t = triplet, q = quartet, br = broad, m = multiplet), integration, coupling constant (Hz). Low-resolution mass spectra were obtained on an Agilent 1200 series 6130 mass spectrometer (Agilent, Santa Clara, CA). High-resolution mass spectra were recorded on a Waters Q-TOF API-US (Waters, Millford, MA). Analytical thin-layer chromatography was performed on Analtech silica gel GF 250-μm plates (Analtech, Newark, DE). Analytical high-performance liquid chromatography (HPLC) was performed on an HP1100 with UV detection at 214 and 254 nm along with ELSD (evaporative light scattering detector) detection, liquid chromatographic-tandem mass spectrometry analysis (LC/MS/MS) (J-Sphere80-C18, 3.0 × 50 mm, 4.1-minute gradient, 5%[0.05% TFA(trifluoroacetic acid)/CH_3CN]:95%[0.05% TFA/H_2O] to 100%[0.05%TFA/CH_3CN]. Preparative reverse phase HPLC purification was performed on a custom HP1100 automated purification system with collection triggered by mass detection or using a Gilson Inc. (Middleton, WI) preparative UV-based system using a Phenomenex Luna C18 column (50 × 30 mm I.D. [internal diameter], 5 μm; Phenomenex, Torrance, CA) with an acetonitrile (unmodified)-water (0.1% TFA) custom gradient. Normal-phase silica gel preparative purification was performed using an automated Combi-flash companion from ISCO (Lincoln, NE). Solvents for extraction, washing, and chromatography were HPLC grade.

Downloaded from dmd.aspetjournals.org at ASPET Journals on March 14, 2015

All reagents were purchased from Sigma Aldrich Chemical Co. and were used without purification. All polymer-supported reagents were purchased from Argonaut Technologies (Redwood City, CA) and Biotage (Uppsala, Sweden). Individual compound synthetic methods are contained in the Supplemental Material.

Cell Culture and Mutagenesis

Human embryonic kidney cell line (HEK293A) cells lines stably expressing rat $mGlu_5$ were maintained in complete DMEM supplemented with 10% FBS, 2 mM L-glutamine, 20 mM HEPES, 0.1 mM nonessential amino acids, 1 mM sodium pyruvate, antibiotic-antimycotic, and G418 (500 μg/ml; Mediatech, Manassas, VA) at 37°C in a humidified incubator containing 5% CO_2, 95% O_2. Point mutations in rat $mGlu_5$-pCl:Neo were generated using a site-directed mutagenesis kit (Quikchange II; Agilent), and mutant plasmids were fully sequenced to verify the desired mutations. HEK293A cells were transfected with the mutant plasmids using Fugene6 (Promega, Madison, WI), and the cells were maintained under 1 mg/ml G418 selection for 2 weeks to obtain the stable cell lines expressing these mutants. Stable polyclonal mutant rat $mGlu_5$ cells and HEK293A cells stably expressing rat $mGlu_1$ were maintained in the same media as the $mGlu_5$ wild-type cells. HEK293A cells stably expressing G-protein–coupled inwardly rectifying potassium channels (HEK293A-GIRK) and the individual group II and group III mGlus were maintained in growth media containing 45% DMEM, 45% F-12, 10% FBS, 20 mM HEPES, 2 mM L-glutamine, antibiotic/antimycotic, nonessential amino acids, 700 μg/ml G418, and 0.6 μg/ml puromycin.

Fluorescence-Based Calcium Assays in Rat $mGlu_5$ Cells

Measurement of $mGlu_5$-mediated intracellular Ca^{2+} mobilization was performed using the Ca^{2+}-sensitive dye Fluo-4 and a Flexstation II (Molecular Devices, Sunnyvale, CA), as described previously (Noetzel et al., 2012). HEK293A cells expressing either $mGlu_5$ wild-type or $mGlu_5$ mutants were incubated with test compound for 60 seconds before stimulation with glutamate. Baseline fluorescence was subtracted from peak fluorescence before normalization to the maximal peak response elicited by glutamate alone (10–100 μM). Data were transformed and fitted using GraphPad Prism 5.0 (GraphPad Software, Inc., San Diego, CA).

Fluorescence-Based Calcium Assays in Rat Astrocytes

Rat cortical astrocytes were plated in 384-well poly-D-lysine coated, black-walled, clear-bottomed plates (BD Falcon, San Jose, CA) in a 20-μl volume of astrocyte growth medium at a density of approximately 15,000–20,000 cells/well and supplemented the following day with G5 diluted 1:100 in astrocyte growth medium. On the day of the experiment, concentration-response curves (CRCs) of test compounds were prepared. Stock compounds were made in dimethylsulfoxide (DMSO) at a concentration of 10 mM. CRCs were made at a 2× concentration in assay buffer (Hanks' balanced salt solution, 20 mM HEPES, 2.5 mM probenecid, pH 7.4) to achieve final concentrations in the assay that ranged from 0.37 nM to 30 μM in an 11-point curve and a final DMSO concentration of 0.3%. Each curve occurred in triplicate in each plate along with vehicle-matched controls. CRCs were generated using a Labcyte Echo 555 employed with Labcyte Dose Response Software package (Labcyte, Sunnyvale, CA). Calcium flux was measured using the Functional Drug Screening System 6000 (FDSS 6000, Hamamatsu, Japan); compound alone was added at 3 seconds to detect any agonist activity, followed by a EC_{20} of glutamate at 143 seconds, and finally a EC_{80} glutamate at 240 seconds. A glutamate concentration (60 μM) resulting in a maximal response was also added in the third addition to wells not receiving compound or previous glutamate additions. The resulting EC_{max} response was used to normalize test responses during data analysis. FDSS data were analyzed using a Microsoft Excel analysis template using Excel formulas for data reduction and IDBS XLfit (Guildford, UK) for curve fitting. Each point was normalized to the initial value for that well (static ratio). For each window (agonist, potentiator, antagonist), the peak static ratio response was determined and corrected by subtraction of the minimum response at the beginning of the data collection. Each corrected response was then expressed as a percentage of the average baseline corrected static ratio of the EC_{max}. For the agonist, potentiator, and antagonist windows, each corresponding $\%EC_{max}$ response was plotted versus the log of the molar concentration of test compound. The data were fit to a four-parameter logistic equation to determine the minimum response, maximum response (percentage response achieved relative to the maximal response obtained with glutamate, $\%\ Glu_{max}$), the log concentration giving the half-maximal response (log EC_{50}), and the slope factor of the curve.

$mGlu_1$ Selectivity Screening

HEK293A cells stably expressing rat $mGlu_1$ were plated in black-walled, clear-bottomed, poly-D-lysine coated 384-well plates (Greiner Bio-One, Monroe, NC) in assay medium at a density of 20,000 cells/well for 24 hours before the assay. Assays were performed at the Vanderbilt University High-Throughput Screening Center as described previously (Hammond et al., 2010; Rodriguez et al., 2010). Calcium flux was measured using the FDSS 6000; vehicle or a fixed concentration of test compound (10 μM) was added, followed by a CRC to glutamate 2.5 minutes later. The change in relative fluorescence over basal was calculated before normalization to the maximal response to glutamate.

Group II and Group III mGlu Selectivity Screening

Test compound activity at the rat group II and III mGlus was assessed using thallium flux through GIRK channels as previously described in detail (Niswender et al., 2008; Hammond et al., 2010). Briefly, HEK293A-GIRK cells expressing mGlu subtypes (2, 3, 4, 6, 7, or 8) were plated into 384-well, black-walled, clear-bottom poly-D-lysine coated plates at a density of 15,000 cells/well in assay medium the day before the assay. On the day of the assay, the medium was aspirated and replaced with assay buffer (Hanks' balanced salt solution, 20 mM HEPES, pH 7.4) supplemented with 0.16 μM Fluozin2-AM (Invitrogen). For these assays, vehicle or fixed concentration of test compound (10 μM) was added, followed by a CRC to glutamate (or L-AP4 in the case of $mGlu_7$) diluted in thallium buffer (125 mM $NaHCO_3$, 1 mM $MgSO_4$, 1.8 mM $CaSO_4$, 5 mM glucose, 12 mM thallium sulfate, 10 mM HEPES), and fluorescence was measured using an FDSS 6000. Data were analyzed as described previously (Niswender et al., 2008). The presence of activity at each receptor was determined by comparing the fold shift imparted by the compound (EC_{50} of glutamate under control conditions divided by EC_{50} in the presence of compound), as well as the effect on the maximum response of glutamate. A compound was determined to be a PAM if it resulted in a fold shift of 2.0 or greater, a NAM if it decreased the maximum response from 100% to 75% or less, and an antagonist if it resulted in a fold shift of 0.5 or less and the maximum response remained above 75%.

Ancillary Pharmacology Screening

VU0403602 was sent to Ricerca Biosciences (Painesville, OH) for testing in their LeadProfiling Screen, a panel of ancillary pharmacology binding assays measuring the percentage of displacement of an orthosteric radioligand at 66 distinct molecular targets. Two independent determinations were made using 10 μM test compound concentration. Significant activity was defined as >50% inhibition of binding at any target. Additionally, a functional human serotonin $5\text{-}HT_{2B}$ assay was performed using rat stomach fundus ($n = 2$) and a 30 μM test compound concentration.

Radioligand Binding Assays

The allosteric antagonist MPEP analog [^{3}H]methoxyPEPy (Cosford et al., 2003) was used to evaluate the interaction of the test compounds with the allosteric MPEP site on $mGlu_5$. Membranes were prepared from HEK293A cells stably expressing rat $mGlu_5$. Compounds were diluted into assay buffer (50 mM Tris and 0.9% NaCl, pH 7.4) to a 2× stock, and 125 μl of test compound was added to each well of a 96-well assay plate; 100-μl aliquots of membranes diluted in assay buffer (50 μg/well) were added to each well. Twenty-five microliters of [^{3}H]methoxyPEPy (5 nM final concentration in assay buffer) was added, and the reaction was incubated at room temperature for 60 minutes with shaking. After the incubation period, the membrane-bound ligand was separated from free ligand by filtration through glass fiber 96-well filter plates (Unifilter-96, GF/B; PerkinElmer Life and Analytical Sciences, Boston, MA). The contents of each well were transferred simultaneously to the

Downloaded from dmd.aspetjournals.org at ASPET Journals on March 14, 2015

filter plate and washed three times with assay buffer (Brandel cell harvester; Brandel Inc., Gaithersburg, MD). Forty microliters of scintillation fluid was added to each well, and the membrane-bound radioactivity was determined by scintillation counting (TopCount; PerkinElmer Life and Analytical Sciences). Nonspecific binding was estimated using 10 μM MPEP.

Animal Use

All animal studies and experiments were conducted in accordance with the National Institutes of Health's *Guide for the Care and Use of Laboratory Animals* and were approved by the *Institutional Animal Care and Use Committee*. Animals were housed under a 12-hour light/dark cycle with access to food and water (ad libitum).

Electrophysiology

Extracellular Field Potential Recordings. In the LTD experiments, 4- to 6-week-old male Sprague-Dawley rats (Charles River, Wilmington, MA) were sacrificed and the brains quickly removed and submerged into ice-cold cutting solution (in mM: 110 sucrose, 60 NaCl, 3 KCl, 1.25 NaH_2PO_4, 28 $NaHCO_3$, 5 D-glucose, 0.6 (+)-sodium-L-ascorbate, 0.5 $CaCl_2$, 7 $MgCl_2$) continuously bubbled with 95% O_2/5% CO_2. Then 400-μm transverse brain slices were made using a vibratome (Leica VT100S; Leica Microsystems, Nussloch, Germany). Individual hippocampi were microdissected from the slice and transferred to a room temperature mixture containing equal volumes of cutting solution and artificial cerebrospinal fluid (ACSF; in mM: 125 NaCl, 2.5 KCl, 1.25 NaH_2PO_4, 25 $NaHCO_3$, 25 glucose, 2 $CaCl_2$, 1 $MgCl_2$) and allowed to equilibrate for 30 minutes. The hippocampi were then transferred to ACSF continuously bubbled with 95% O_2/5% CO_2 for a minimum of an additional hour. For recordings, the slices were transferred to a submersion recording chamber and allowed to equilibrate for 5–10 minutes at 30–32°C with a flow rate of 2 ml/min. Schaffer collaterals were stimulated by placing a bipolar-stimulating electrode in the stratum radiatum near the CA3-CA1 border. Recording electrodes were pulled with a Flaming/Brown micropipette puller (Sutter Instruments, Novato, CA), filled with ACSF, and placed in the stratum radiatum of area CA1. Field potential recordings were acquired using a MultiClamp 700B amplifier (Molecular Devices, Sunnyvale, CA) and pClamp 10 software (Molecular Devices). Input-output curves were generated to determine the stimulus intensity that produced 50%–60% of the maximum field excitatory postsynaptic potential (fEPSP) slope before each experiment, which was then used as the baseline stimulation. Test compounds were diluted to the appropriate concentrations in DMSO (0.1% final) in ACSF and applied to the bath for 10 minutes using a perfusion system. Chemically induced mGlu LTD was initiated by the application of DHPG in ACSF (75 μM) for 10 minutes. Sampled data were analyzed offline using Clampfit 10. The slopes from three sequential fEPSPs were averaged. All fEPSP slopes were normalized to the average slope calculated during the predrug period (percentage of baseline). Data were analyzed using GraphPad Prism.

Epileptiform Experiments. Male Sprague-Dawley rats (24–30 days old, Charles River) were sacrificed and the brains quickly removed and submerged into ice-cold cutting solution (as described above) continuously bubbled with 95% O_2/5% CO_2. Then 400-μm transverse slices were made as described above. Individual hippocampi were transferred to artificial cerebrospinal fluid (ACSF, in mM: 124 NaCl, 5 KCl, 1.25 NaH_2PO_4, 26 $NaHCO_3$, 10 glucose, 2 $CaCl_2$, 1.2 $MgCl_2$), maintained at room temperature, and allowed to equilibrate for a minimum of 1 hour. For recordings, the slices were transferred to a submersion recording chamber and allowed to equilibrate for 5–10 minutes at 30–32°C with a flow rate of 2 ml/min. Recording electrodes were pulled with a Flaming/Brown micropipette puller (Sutter Instruments, CA), filled with ACSF and placed in the cell body layer of CA3. Field potential recordings (spontaneous events) were acquired using a MultiClamp 700B amplifier (Molecular Devices) and pClamp10 software (Molecular Devices). Compounds of interest were diluted to the appropriate concentrations in DMSO (0.1% final) in ACSF and applied to the bath for 10 minutes using a perfusion system. DHPG was used as a positive control (50 μM). Sampled data were analyzed offline using MiniAnalysis (Synaptosoft Inc., Fort Lee, NJ) to determine the amplitude and interevent interval of the spontaneous events and normalized to the predrug period.

Plasma Protein Binding and Nonspecific Binding in Brain Homogenate

The extent of plasma protein binding and nonspecific binding of test compounds was determined in vitro in male (Sprague-Dawley) rat plasma and brain homogenate via rapid equilibrium dialysis (RED; ThermoFisher Scientific, Rochester, NY). A 96 well plate containing plasma and an individual test article (5 μM) was vortex mixed. A portion (200 μl) of the mixture was transferred to the *cis*-chamber of the RED insert and dialyzed against phosphate buffer (350 μl, 25 mM, pH 7.4) in the *trans*-chamber and incubated (37°C) with shaking (4 hours). After the incubation, an aliquot from each chamber was diluted (1:1; v/v) with either plasma or buffer from the *cis*- or *trans*-chamber, respectively, and transferred to a new 96-well plate. Protein precipitation of the matrices was executed by the addition of ice-cold acetonitrile containing carbamazepine (50 nM) as an internal standard for LC-MS/MS analysis. The plate was centrifuged [3000 relative centrifugal force (RCF), 10 minutes] and the supernatants transferred to a new 96-well plate, where they were diluted in H_2O (1:1; v/v). The plate was then sealed for LC/MS/MS analysis.

Hepatic Microsome Stability Assessment of VU0403602

The metabolic stability of VU0403602 was investigated in male S-D rat hepatic microsomes using substrate depletion methods (percentage of parent compound remaining). In a 96-well plate, a potassium phosphate-buffered (0.1 M, pH 7.4) solution of VU0403602 (1 μM), microsomes (0.5 mg/ml), + NADPH (1 mM), + $MgCl_2$ (3 mM) was incubated at 37°C under ambient oxygenation; reactions were initiated by the addition of NADPH. At designated times (t = 0, 3, 7, 15, 25, and 45 minutes), an aliquot of the incubation mixture was removed and precipitated by the addition of two volumes of ice-cold acetonitrile containing carbamazepine as an internal standard (50 ng/ml). The plates were centrifuged at 3000 RCF (4°C) for 10 minutes. The resulting supernatants were diluted 1:1 (supernatant: water) into a new 96-well plates in preparation for LC/MS/MS analysis. The compound was assayed in triplicate within the same 96-well plate. The substrate depletion method previously described was used to estimate the in vitro intrinsic clearance (CL_{int}; ml/min per kilogram) of VU0403602 in rat liver microsomes (Obach and Reed-Hagen, 2002).

Hepatic Biotransformation of VU0403602

The in vitro metabolism of VU0403602 was investigated in hepatic S9 fractions from S-D rats (male, pooled; BD Biosciences, San Jose, CA). A potassium phosphate-buffered solution (0.1 M, pH 7.4) of test compound (25 μM) and hepatic S9 fractions (5 mg/ml) was incubated (37°C) in borosilicate glass tubes under ambient oxygenation for 1 hour with select reactions being fortified with NADPH (2 mM), UDGPA (2 mM), and/or adenosine 3′-phosphate 5′-phosphosulfate lithium salt hydrate (2 mM). Protein was precipitated by the addition of two volumes of acetonitrile with subsequent centrifugation (3000 RCF, 10 minutes). The supernatant was dried under a stream of nitrogen gas and reconstituted in 85:15 (v/v) ammonium formate (10 mM, pH 4.1, aqueous):acetonitrile in preparation for LC/MS/MS analysis. In an identical manner, and where indicated, the metabolism of VU0403602 was investigated in Sprague-Dawley rat intestinal S9 fractions (4 mg/ml, pooled male S-D rats, BD Biosciences).

Pharmacokinetic Studies in Rats after Intravenous Administration

Male Sprague-Dawley rats (250–300 g) were purchased from Harlan Laboratories (Indianapolis, IN). Catheters were surgically implanted in the carotid artery and jugular vein. The cannulated animals were acclimated to their environment for approximately 1 week before dosing. Parenteral administration of test compounds to rats was achieved via a jugular vein catheter at a dose of 1 or 3 mg/kg and a dose volume of 1 ml/kg [10% ethanol (EtOH)/50% PEG (polyethylene glycol) 400/40% saline] or 3 ml/kg (10% EtOH/90% PEG 400) for metabolite M1 and parent VU0403602, respectively. Blood collections via the carotid artery were performed at 2, 7, 15, and 30 minutes and 1, 2, 4, 7, and 24 hours postadministration. Samples were collected into chilled, EDTA-fortified tubes, centrifuged for 10 minutes (3000 RCF, 4°C), and the resulting plasma stored at −80°C until analysis. Pharmacokinetic parameters were obtained from noncompartmental analysis (NCA, WinNonLin, v5.3; Pharsight

Downloaded from dmd.aspetjournals.org at ASPET Journals on March 14, 2015

Corp., Mountain View, CA) of individual animal concentration-time profiles following the parenteral administration of a test compound.

Determination of Systemic and CNS Exposure of VU0403602

Male Sprague-Dawley rats (250–300 g) were purchased from Harlan Laboratories and acclimated to their surroundings for approximately 1 week before dosing. Administration (i.p.) of test compounds to rats was performed at various doses (3–30 mg/kg). When warranted, rats received pretreatment with ABT (PO, 50 mg/kg) or coadministration of test article and MPEP (i.p., 5 or 10 mg/kg) (Balani et al., 2002). Plasma and whole brains were collected at varied time points using nonserial sampling methods from multiple animals. Plasma samples were collected into chilled, EDTA-fortified tubes and centrifuged for 10 minutes (3000 RCF, 4°C), and the resulting plasma stored at −80°C until analysis. Brain samples were rinsed with cold phosphate-buffered saline, snap frozen (dry ice), and stored at −80°C until LC/MS/MS analysis. Plasma and brain time-concentration area-under-the-curves (AUCs) were calculated by the trapezoidal method employing Prism software (GraphPad).

Behavioral Manifestations of Seizure Activity

To study $mGlu_5$ PAM-induced behavioral manifestation of seizure activity, rats received various doses (i.p., 30 mg/kg) of the test compound with or without the $mGlu_5$ antagonist MPEP (5 and 10 mg/kg). Compounds were formulated in 10% Tween 80 and administered at a volume of 3 ml/kg. Animals were monitored continuously for 2 hours. After this procedure, rats were euthanized and brains removed and processed for compound exposure levels. Rats were scored for behavioral manifestations of seizure activity in periods of 5 minutes, once every 5 minutes for the first 15 minutes, then once every 15 minutes up to 1 hour, and every 30 minutes up to 2 hours. Compound-induced behavioral manifestations of seizures were scored using a five-grade modified Racine scoring system (Rook et al., 2012). A score of 0 represents no behavioral alteration; score 1, immobility, mouth and facial movements, facial clonus; score 2, head nodding, forelimb and/or tail extension, rigid posture; score 3, forelimb clonus, repetitive movements; score 4, rearing, forelimb clonus with rearing, rearing and falling; and score 5, continuous rearing and falling, jumping, severe tonic-clonic seizures.

Reversal of Amphetamine-Induced Hyperlocomotion

Studies were conducted using male Sprague-Dawley rats purchased from Harlan Laboratories weighing 275–300 g. Dose groups consisted of 5 to 12 rats per group. VU0403602 was dissolved in 10% Tween 80 and double-deionized water, and the pH was adjusted to approximately 7.0 using 1 N NaOH. VU0403602 was administered i.p. at a dose of 3, 10, or 30 mg/kg in a 3 ml/kg volume. Studies were performed as previously described (Noetzel et al., 2012). Briefly, rats were placed in the open-field chambers and allowed to habituate for 30 minutes, followed by pretreatment (i.p.) with vehicle or test compound. After an additional 30 minutes, rats received a saline vehicle or 1 mg/kg amphetamine via s.c. injection. Locomotor activity was measured for an additional 60 minutes. Ambulation or locomotor activity was measured as the number of total photobeam breaks per 5-minute interval using Motor Monitor System software (Kinder Scientific, Poway, CA). Main effects of test compound treatment on the amphetamine-induced locomotor activity area under the time-course curve were evaluated using one-way analysis of variance. Comparisons of treatment group effects relative to the vehicle + amphetamine group were completed across the time interval from $t = 60$ to 120 minutes using Dunnett's post hoc tests with a P value < 0.05 considered significant.

Liquid Chromatography-UV-Mass Spectrometry Analysis of VU0403602 and Corresponding Metabolites

Plasma and brain tissue samples originating from in vivo studies were analyzed with electrospray ionization by an AB Sciex Q-TRAP 5500 (Foster City, CA) that was coupled to a Shimadzu LC-20AD pump (Columbia, MD) and a Leap Technologies CTC PAL auto-sampler (Carrboro, NC). Analytes were separated by gradient elution using a C18 column (3 × 50 mm, 3 μm; Fortis Technologies Ltd, Cheshire, UK) that was thermostated at 40°C. HPLC mobile phase A was 0.1% formic acid in water (pH unadjusted); mobile phase B was 0.1% formic acid in acetonitrile (pH unadjusted). A 30% B gradient was held for 0.2 minute and was linearly increased to 90% B over 0.8 minute, with an isocratic hold for 0.6 minute, before transitioning to 30% B over 0.1 minute. The column was re-equilibrated (1 minute) before the next sample injection. The total run time was 2.5 minutes, and the HPLC flow rate was 0.5 ml/min. The source temperature was set at 500°C, and mass spectral analyses were performed using multiple-reaction monitoring of transitions specific for the test articles and metabolites and using a Turbo-Ionspray source in positive ionization mode (5.0-kV spray voltage). All data were analyzed using AB Sciex Analyst 1.5.1 software. The lower limits of quantitation for VU0403602, VU0453103 (M1), and VU0451326 (M2), were determined at 1 ng/ml in plasma and 0.5 ng/g in brain homogenates.

Samples from in vitro DMPK assays (CL_{int}, plasma protein and brain homogenate binding), were analyzed on a TSQ Quantum Ultra (Thermo Fisher Scientific, Waltham, MA) using electrospray ionization (ESI). The mass spectrometer was coupled to an Accella HPLC pump system (Thermo Fisher Scientific) and a CTC PAL autosampler. Analytes were separated by gradient elution employing two Acquity BEH C18 columns (2.1 × 50 mm, 1.7 μ; Waters Corp., Milford, MA) that were heated at 50°C. HPLC mobile phase A was a 95:5:0.1 mixture of water/acetonitrile:formic acid, respectively; mobile phase B was a 95:5:0.1 mixture of acetonitrile/water/formic acid, respectively. The following was the gradient program that was used in these separations: pump 1 ran the gradient: 95:5 (A:B) at 800 μl/min hold 0 to 0.5 minute, linear ramp to 5:95 (A:B) 0.5 to 1.0min, 5:95 (A:B) hold 1.0 to 1.9 minutes, return to 95:5 (A:B) at 1.9 minutes. While pump 1 ran the gradient method, pump 2 equilibrated the previously used column under isocratic conditions (95:5; A:B). The total run time was 2.0 minutes. All compounds were optimized and analyzed using QuickQuan (Thermo Fisher Scientific) software.

Samples from in vitro metabolism experiments and authentic standards of test compound/metabolites were analyzed on an Agilent 1100 HPLC system employing a Supelco Discovery C18 column (2.1 × 150 mm, 5 μm; Sigma-Aldrich Chemical Company). Solvent A was 10 mM (pH 4.1) ammonium formate and solvent B was acetonitrile. The initial mobile phase was 15% and by linear gradient transitioned to 80% over 20 minutes. The flow rate was 0.400 ml/min. The HPLC eluent was first introduced into an Agilent 1100 DAD (single wavelength selected, 254 nM), followed by electrospray ionization introduction into a Finnigan LCQ Deca XP^{PLUS} ion trap mass spectrometer (Thermo Fisher Scientific) operated in either the positive or negative ionization mode. Ionization was assisted with sheath and auxiliary gas (ultrapure nitrogen) set at 60 and 40 psi, respectively. The electrospray voltage was set at 5 kV with the heated ion transfer capillary set at 300°C and 30 V. Relative collision energies of 25%–35% were used when the ion trap mass spectrometer was operated in the MS/MS or MS^n mode.

Results

VU0403602 Displays a Mixed $mGlu_5$ Agonist-PAM Pharmacology Profile In Vitro

We previously reported a series of small-molecule selective $mGlu_5$ PAMs that were developed based on a biaryl acetylene scaffold; a number of highly potent compounds were identified that display in vivo activity in rodent behavioral models of antipsychotic efficacy (Williams et al., 2011; Rook et al., 2012). We recently identified a cyclobutyl picolinamide analog, VU0403602, that displayed potent $mGlu_5$ agonist (31.1 nM, 49% Glu_{max}) and PAM (4 nM, 100% Glu_{max}) activity in vitro (Fig. 2), inducing a progressive concentration-dependent left-shift (9-fold maximal shift at 1 μM, data not shown) of the glutamate CRC in a functional calcium mobilization assay in $mGlu_5$-expressing HEK293A cells (Gregory et al., 2013). Importantly, VU0403602 is absent of activity at $mGlu_1$ (Ca^{2+} assay), group II (GIRK thallium flux assay), and group III receptors (GIRK thallium flux assay), indicating that the compound is a subtype-selective $mGlu_5$ ligand (Supplemental Fig. 1). VU0403602 displayed minimal off-target ancillary pharmacology, as radioligand binding displacement of a broad panel (>65) of GPCRs, ion channels, transporters, and other targets ($n = 2$, 10 μM test compound) indicated significant activity (>50%) for only three targets: human norepinephrine transporter

Downloaded from dmd.aspetjournals.org at ASPET Journals on March 14, 2015

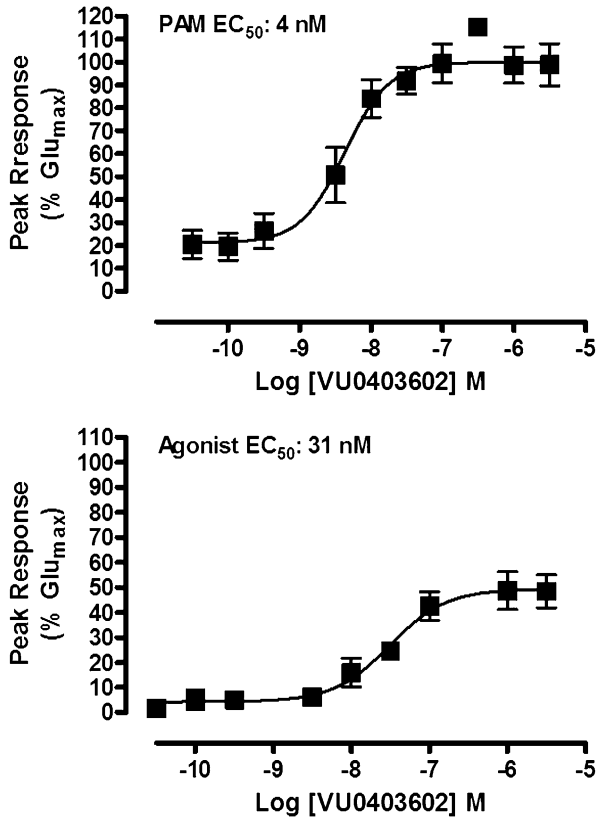

Fig. 2. VU0403602 is a potent positive allosteric modulator of $mGlu_5$ with direct agonist activity in the absence of glutamate in vitro. VU0403602 causes concentration-dependent increases in the mobilization of intracellular calcium in recombinant cells expressing $mGlu_5$ in the presence (top) and absence (bottom) of a fixed submaximal ($\sim EC_{20}$) concentration of glutamate and with a PAM EC_{50} of 4 nM (100% response achieved relative to the maximal response obtained with glutamate, % Glu_{max}) and an agonist EC_{50} of 31.1 nM (49.4% Glu_{max}). Data represent the mean ± S.E.M. of four independent experiments performed in duplicate.

(66% inhibition), human dopamine transporter (DAT, 67% inhibition), and a human serotonin receptor (5-HT_{2B}, 92% inhibition). Subsequent 5-HT_{2B} functional assays with VU0403602 (30 μM) in rat stomach fundus tissue revealed no significant activity (data not shown).

Competition binding experiments using the MPEP site radioligand [^{3}H]-mPEPy to label membranes from rat mGlu5-expressing HEK cells revealed a fully competitive interaction by VU0403602, similar to that of the unlabeled MPEP control (Supplemental Fig. 2). In additional cell-based functional experiments using $mGlu_5$-expressing cells, CRCs of VU0403602 in the presence of multiple fixed concentrations of the noncompetitive $mGlu_5$ antagonist, 5PMEP (occupies the MPEP allosteric site), exhibited parallel right shifts, with a corresponding Schild regression analysis indicating a competitive mode of interaction (slope = 1.06)). These data support a fully competitive interaction of VU0403602 at the prototypical MPEP binding site of $mGlu_5$.

In Vivo Administration of VU0403602 Induces Adverse Events in Rats

Although VU0403602 produced a dose-dependent (3, 10, 30, mg/kg, i.p.; ED_{50}, 21 mg/kg) efficacy in the reduction of hyperlocomotion in Sprague-Dawley rats (Supplemental Fig. 3) receiving amphetamine (1 mg/kg, s.c.), the systemic administration of this $mGlu_5$ PAM also induced pronounced AEs marked by the onset of seizures, forelimb asymmetry, tremor, and facial bleeding, the severity of which were recorded using the Racine assessment method (Rook et al., 2012). The onset of VU0403602-mediated AEs was similar to those observed in S-D rats that received a single administration (i.p.) of the Ago-PAM VU0424465 (agonist EC_{50}: 171 nM, 65% Glu_{max}, PAM EC_{50}: 2 nM, 88% Glu_{max}; Rook et al., 2012). When rats received a single i.p. dose (30 mg/kg) of VU0403602 in the absence of amphetamine, subsequent observations revealed a time-dependent manifestation of the aforementioned behavioral effects (Fig. 3). To determine whether the AEs observed in rats were $mGlu_5$ target-mediated, we administered (i.p.) VU0403602 (30 mg/kg) with the $mGlu_5$ allosteric antagonist, MPEP (5 and 10 mg/kg) and monitored the behavioral effects for 4 hours post-treatment. The lower dose (5 mg/kg) of MPEP reduced the severity of the VU0403602-induced behavioral AEs by approximately 50%, whereas rats receiving the 10 mg/kg dose of MPEP were completely devoid of the behavioral manifestations (Fig. 3). These data implicate a role for $mGlu_5$ in the mechanism underlying the AEs resulting from the administration of VU0403602. Interestingly, pretreatment of rats with the pan cytochrome P450 inactivator, 1-aminobenzotriazole (ABT; 50 mg/kg, i.p.), completely mitigated the onset of the behavioral AEs resulting from the systemic administration of VU0403602, indicating that one or more metabolites of this PAM may be contributing to the $mGlu_5$-mediated toxicity observed in vivo (Fig. 3) (Balani et al., 2002).

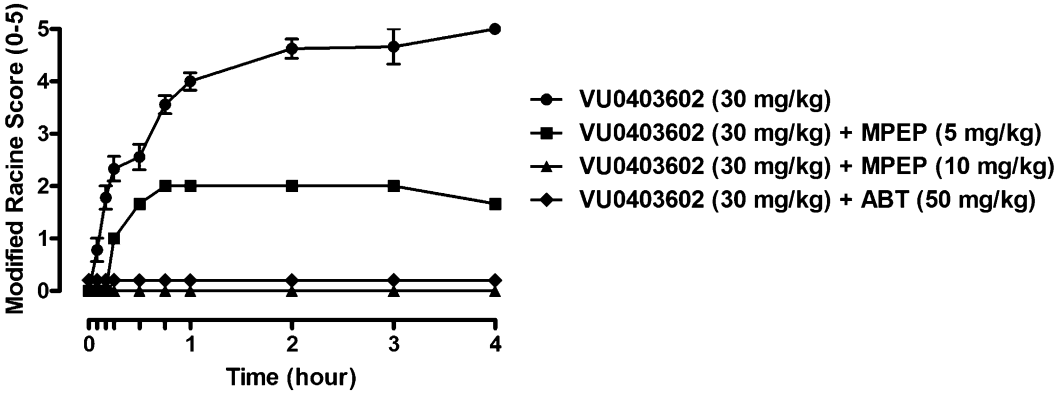

Fig. 3. The $mGlu_5$ ago-PAM VU0403602 induces time-dependent increases in behavioral convulsions, which are mitigated by pretreatment with the $mGlu_5$ antagonist MPEP or the P450 inactivator ABT in male Sprague-Dawley rats. VU0403602 administration (i.p., 30 mg/kg, $n = 9$) causes full clonic-tonic seizure activity (modified Racine score 5); the same administration of VU0403602 to rats pretreated with a lower dose of MPEP (i.p., 5 mg/kg, $n = 3$) or a higher dose of MPEP (i.p., 10 mg/kg, $n = 3$) reduced (modified Racine score 2) or completely blocked (modified Racine score 0), respectively, the severity of seizure activity. In rats pretreated with ABT (PO, 50 mg/kg, $n = 6$), administration of VU0403602 (i.p., 30 mg/kg) failed to induce any seizure activity (modified Racine score 0). Data represent mean ± S.E.M.

Downloaded from dmd.aspetjournals.org at ASPET Journals on March 14, 2015

In Vitro and In Vivo Disposition of VU0403602 in Sprague-Dawley Rats Reveals Hepatic Metabolism as the Mechanism of Clearance

After the initial rat behavioral findings, the DMPK profile of VU0403602 was determined using conventional in vitro subcellular fraction metabolism and in vivo dosing paradigms to define the biotransformation pathways for VU0403602 and the contribution(s) of metabolites toward precipitating AEs in rat (Balani et al., 2005). The CL_{int} of VU0403602 was assessed in rat hepatic microsomes and subsequently used to predict the extent of hepatic clearance in vivo. The CL_{int} and hepatic clearance values (271 ml/min per kilogram and 55.6 ml/min per kilogram, respectively) for VU0403602 correlated well with the total body plasma clearance value (CL_p: 36.2 ml/min per kilogram) observed in rats after parenteral administration (3 mg/kg) (Supplemental Fig. 4), indicating that hepatic metabolism was likely the predominant mechanism of clearance for VU0403602. Consistent with this assessment, we detected negligible amounts of unchanged VU0403602 excreted in the urine. The volume of distribution estimated at steady state of VU0403602 (V_{ss}, 6.73 l/kg) exceeded that of the total body water in rats and, coupled with its moderate CL_p in vivo, resulted in a mean residence time of approximately 3 hours (Supplemental Fig. 4). In vitro rapid equilibrium dialysis (RED) indicated the plasma protein binding of VU0403602 to be extensive in rat plasma, producing a corresponding fraction unbound (F_u) of < 0.01; RED data also indicated extensive nonspecific binding of VU0403602 ($F_u < 0.01$) in rat brain homogenates.

In Vitro Biotransformation of VU0403602 Results in the Formation of Two Principal Metabolites

LC/MS/MS was used to characterize the metabolites of VU0403602 produced in vitro from rat S9 fractions (intestinal, hepatic, brain), potentially representing metabolite-ligands of $mGlu_5$ that could contribute to the AEs observed in rats. Data from these experiments revealed two principal biotransformation pathways for VU0403602 (Scheme 1), NADPH-dependent oxidation of the cyclobutyl moiety of VU0403602 to the hydroxylated metabolite, M1, and the NADPH-independent amide hydrolysis of VU0403602 to the carboxylic acid metabolite, M2. Metabolite M1 was observed at approximately 16.1 minutes as the $[M + H]^+$ at *m/z* 311 (Fig. 4). The primary fragmentation observed (100% relative) was the gas phase loss of water (-18 Da; $-H_2O$) to produce the ion at *m/z* 293, representing a 16-Da increase over the water loss fragment observed in the MS/MS of VU0403602 (m/z 277). A secondary fragmentation from the ion at m/z 293 was also observed in the MS/MS of M1 (m/z 275). Another fragmentation observed for M1 was the gas phase, water-assisted fragmentation of the amide bond that resulted in the formation of an ion at m/z 242 (20% relative). The water-assisted amide fragmentation was also observed in the MS/MS of VU0403602, producing a fragment ion at m/z 242 in addition to the loss of the cyclobutyl moiety producing an $[M + 2H]^+$ at m/z 241. The proposed carboxylic acid metabolite M2, observed at 15.7 minutes ($[M + H]^+$ at m/z 242), resulted in the gas phase decarboxylation of M2, producing a fragment ion at m/z 196.

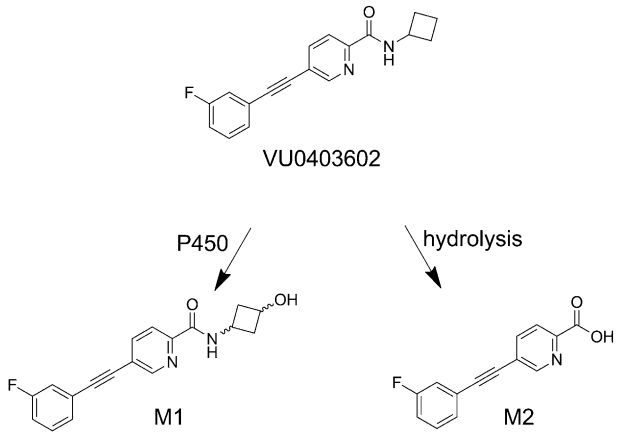

Scheme 1. Principal pathways of VU0403602 metabolism observed in vitro in male Sprague-Dawley rat hepatic S9 fractions.

To determine the relative stereochemistry of oxidation of the cyclobutyl moiety of VU0403602 to the hydroxylated metabolite, M1, we synthetically prepared authentic *cis*- and *trans*-hydroxylated compounds from the ci-s/*trans*-3-hydroxy-1-amino-cyclobutane and a requisite amide coupling; chiral SFC was used to separate the *cis*- and *trans*-standards (Supplemental Schemes 1–3). The *cis*- (VU0453102) and *trans*- (VU0453103) structures were confirmed based on both 1D NMFR studies (Supplemental Figs. 5–8), including the examination of nuclear overhauser effects between the methine protons within the cyclobutane ring system (Supplemental Fig. 9). Subsequent LC/MS/MS analysis confirmed the stereochemistry of M1 as that of the *trans*-compound (i.e., VU0453103) based on the corresponding LC retention time and MS/MS fragmentation pattern. The structure proposed for M2 was also confirmed via LC/MS/MS comparison with its authentic standard (VU0451326).

The Hydroxylated Metabolite (M1) is a Metabolite-Ligand of $mGlu_5$ Displaying Agonist and PAM Activity

A pharmacological characterization of M1 on the $mGlu_5$ receptor was obtained through the use of functional calcium mobilization assays measuring agonist, PAM, and antagonist responses at $mGlu_5$ in recombinant HEK293A cells. In vitro analysis revealed M1 to be a robust ago-PAM, possessing agonist and PAM EC_{50} values of 400 nM (78% Glu_{max}) and 16.9 nM (94% Glu_{max}), respectively (Fig. 5). Related glutamate CRC experiments demonstrated that M1 (10 μM) induced a maximal left shift of 8.2-fold, similar to that of 9-fold for the parent PAM, VU0403602 (1 μM, data not shown). However, unlike the partial $mGlu_5$ agonist activity of the parent VU0403602 (49.4% Glu_{max}), the hydroxylated metabolite M1 displayed a near full agonist activity (94% Glu_{max}). By contrast, the carboxylic acid metabolite (M2) displayed no activity at $mGlu_5$ up to the limit of solubility (agonism, PAM, antagonism EC_{50} values >30 μM, data not shown).

In Vivo Metabolism of VU0403602 Resulted in the Formation and Distribution to the CNS of the Active Metabolite-Ligand M1

Based on the abundant formation in vitro and the potent $mGlu_5$ pharmacological activity observed for M1, we suspected that the systemic formation and CNS exposure of this hydroxylated metabolite in vivo may contribute to the adverse events observed in rats. Moreover, a role of M1 in eliciting the AEs in rats would be consistent with the ABT results, where the absence of AEs was noted in rats that had received the single pretreatment with the P450 inactivator, ABT. Therefore, we administered VU0403602 to rats (i.p., 30 mg/kg; $n = 2$) that were treated with either ABT (PO, 50 mg/kg) or vehicle (0.5% methylcellulose in water) followed by brain and blood collections (1.5 hour postdose) to determine the concentrations of VU0403602 and its metabolites (M1 and M2) in the plasma and CNS (Table 1). The separation of plasma and brain homogenates was first demonstrated with a protracted LC/MS/MS gradient to profile qualitatively the range of metabolites observed in vivo; results from this LC/MS/MS analysis indicated that VU0403602, M1, and M2 were the principal components observed in vivo, with a negligible component observed

Downloaded from dmd.aspetjournals.org at ASPET Journals on March 14, 2015

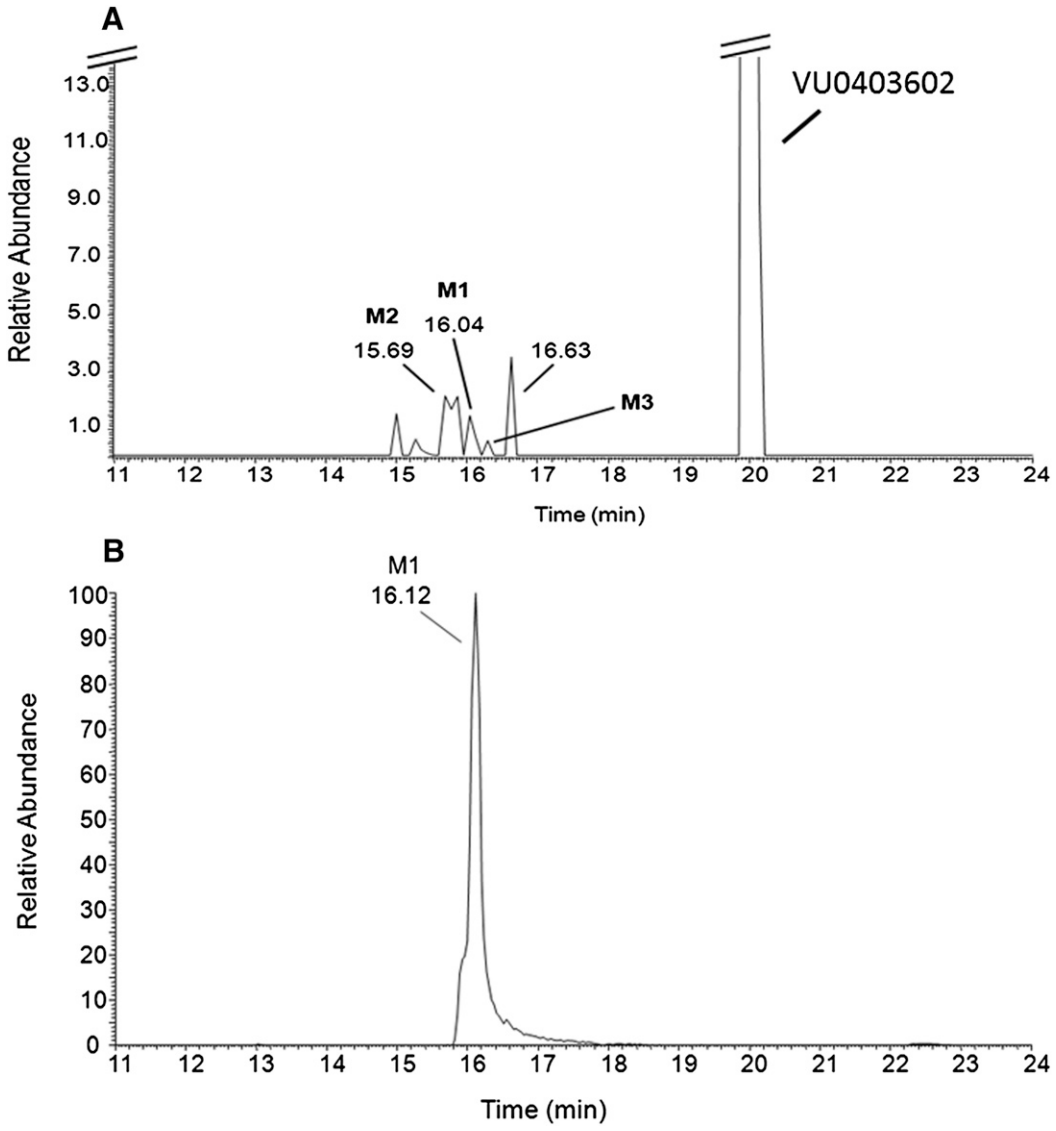

Fig. 4. Representative reconstructed LC/MS/MS total ion current (TIC) (A) of extracts from a Rat hepatic S9 incubation (+NADPH) of VU0403602, showing the principal metabolites M1 and M2, as well as a minor hydroxylated metabolite M3. A corresponding TIC (B) from the LC/MS/MS analysis (MS/MS, m/z 311) of brain extracts from rats receiving a 30 mg/kg dose (i.p.) of VU0403602 reveals M1 to be the principal hydroxylated metabolite in vivo.

representing the *cis*-isomer of M1. Hence, the remaining quantitative bioanalysis of plasma and brain homogenate samples was executed with a standard high-throughput LC/MS/MS gradient as described already herein without the resolution of the *cis*- and *trans*-hydroxylated metabolites. In the absence of ABT, VU0403602 reached an average maximal concentration (C_{max}) of 3.2 μM (5 nM unbound) with a corresponding time to reach C_{max} (T_{max}) of 0.25 hour in plasma; the C_{max} observed in brain was 11.5 μM (6 nM, unbound) with an average T_{max} of 0.88 hour (Table 1). In plasma, M1 reached an average total C_{max} of 64 nM (4 nM unbound) with an average T_{max} of 0.25 hour (Table 1). The brain penetration observed for M1 was substantial, reaching an approximate 9:1 distribution relative to the systemic plasma compartment. M1 reached an average brain C_{max} of 400 nM (4 nM, unbound) and a corresponding T_{max} of 1.5 hours (Table 1). Because of the extensive plasma protein- and nonspecific-binding of VU0403602 ($F_u << 0.01$) and M1 (F_u, 0.01) observed in vitro, the framing of the relevant concentrations observed between the two tissue compartments (i.e., systemic circulation and the CNS) may be most appropriate when considering the total concentrations achieved. Moreover, this framing of concentrations may also be best applied to the pharmacological activity elicited by VU0403602 and M1 in vivo. However, regardless of consideration of total or unbound levels achieved, the results obtained from in vivo analysis are consistent with that generated from the in vitro metabolism experiments; rats that had received the P450 inactivator ABT produced an approximate 11-fold lower C_{max} of the hydroxylated metabolite M1 in plasma (13-fold lower C_{max}, brain) relative to the vehicle control (-ABT) treated rats (Table 1). Likewise, ABT pretreatment also reduced the area-under-the-curve ($AUC_{0\text{-}6h}$) of M1 in plasma by approximately 17-fold in rats receiving a single administration (i.p.) of VU0403602, with a corresponding 8.4-fold reduction in the brain $AUC_{0\text{-}6}$ of M1 (Table 1). Overall, the impact of ABT pretreatment on the metabolism of VU0403602 was profound, resulting in the substantial reduction of M1 exposure in vivo, both in terms of maximal plasma and brain levels and systemic exposure. As expected for a non-P450–mediated biotransformation such as amide hydrolysis, ABT pretreatment had little to no effect on the C_{max} or $AUC_{0\text{-}6h}$ of the carboxylic acid metabolite, M2. Collectively, these data demonstrate the in vivo relevance of the $mGlu_5$ ago-PAM metabolite-ligand, M1, in

Downloaded from dmd.aspetjournals.org at ASPET Journals on March 14, 2015

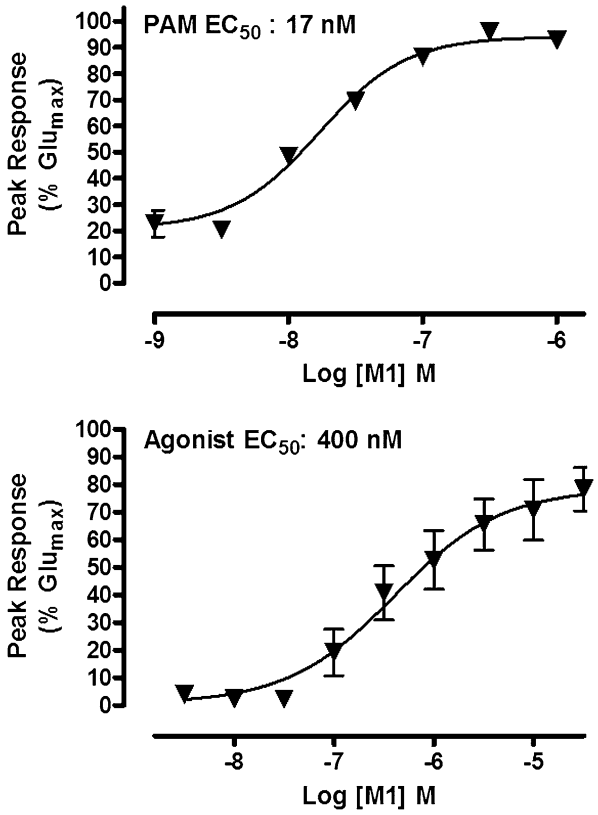

Fig. 5. M1 is a potent positive allosteric modulator of $mGlu_5$ with direct agonist activity in the absence of glutamate in vitro. M1 causes concentration-dependent increases in the mobilization of intracellular calcium in recombinant cells expressing $mGlu_5$ in the presence (top) and absence (bottom) of a fixed submaximal (~EC_{20}) concentration of glutamate and with a PAM EC_{50} of 16.9 nM (94% Glu_{max}) and an agonist EC_{50} of 400 nM (79% Glu_{max}). Data represent the mean ± S.E.M. of at least three independent experiments performed in duplicate.

the onset of adverse behavioral events observed in rats receiving i.p. administration of VU0403602.

In Vitro Rat Brain Slice Electrophysiology

VU0403602 and its Hydroxylated Metabolite M1 Induce Long-Term Depression in Rat Hippocampus. We and others have demonstrated the induction of LTD at the Schaffer-collateral-CA1 (SC-CA1) synapse in the hippocampus as a result of $mGlu_5$ activation by orthosteric agonists as well as allosteric ago-PAMs. Importantly, we have demonstrated that allosteric $mGlu_5$ modulators displaying exclusive PAM pharmacology are incapable of inducing LTD in the absence of an orthosteric ligand (e.g., DHPG). As previously discussed, the allosteric modulator VU0403602 displayed mixed ago-PAM pharmacology at $mGlu_5$ in recombinant cells expressing the rat receptor. To demonstrate the ago-PAM behavior of VU0403602 in a native system, we investigated alterations in electrophysiological responses in rat brain slices following in vitro exposure to VU0403602. Data generated from these experiments indicated that VU0403602 (10 μM) induced pronounced hippocampal LTD at the SC-CA1 synapse (Fig. 6), with a prolonged depression of the fEPSP slope (39.8 ± 5.9% of baseline) well after the compound had been washed from the slice preparation (55 minutes after washout). Likewise, the hydroxylated metabolite M1 (10 μM) also induced significant LTD at the SC-CA1 synapse (Fig. 8) with a similar magnitude of depression of the fEPSP (slope 68.9 ± 4.9% of baseline) and duration of action (55 minutes post washout). (Fig. 6).

VU0403602 and Metabolite M1 Induce Epileptiform Activity in the Rat Hippocampal CA3 Region In Vitro. Having demonstrated that VU0403602 and its principal oxidative metabolite M1 were capable of inducing alterations in LTD, additional experiments investigating whether these ago-PAMs are capable of inducing epileptiform activity in rat hippocampus, specifically in CA3 pyramidal neurons, were performed. Similar to the agonist DHPG, the hydroxylated metabolite M1 (10 μM) and parent VU0403602 (10 μM) induced pronounced epileptiform activity, as evidenced by decreases in the interevent intervals of spontaneous field population spikes (48.1 ± 7.8% and 48.8 ± 11% of baseline, respectively) detected by extracellular field potential recordings in the pyramidal cell body layer of area CA3 in the hippocampal slices (Fig. 7). Similar to the positive control DHPG (50 μM), neither VU0403602 nor M1 significantly affected the amplitude of spontaneous events (Fig. 7). Together, results from the rat hippocampal electrophysiology experiments indicate that the principal oxidative metabolite-ligand M1 is capable of inducing LTD and epileptiform activity in native systems, a finding consistent with $mGlu_5$ activation and one that advances our understanding of the mechanism of AEs observed in rats receiving systemic administration of the parent compound, VU0403602.

Direct Administration of M1 Results in Behavioral AEs in Rats

The systemic administration of M1 to rats was executed to determine whether this $mGlu_5$ metabolite-agonist was capable of

TABLE 1

Pharmacokinetics of VU0403602 and the formation of its principal metabolites (M1, M2) in vivo in male Sprague-Dawley rats after i.p administration (30 mg/kg) in the absence and presence of pretreatment with the cytochrome P450 inactivator 1-aminobenzotriazole (ABT)

Data represent mean values (n = 2).

Analyte	Pretreatment	Plasma C_{max}	Plasma T_{max}	Plasma $AUC_{0\text{-inf}}$	Brain C_{max}	Brain $AUC_{0\text{-inf}}$
		μM	h	$\mu M*h$	μM	$\mu M*h$
VU0403602	—	3.21 (0.005)[a]	0.25	3.63 (0.006)[a]	11.5 (0.006)[b]	7.79 (0.004)[b]
	+ABT	11.0 (0.018)[a]	0.75	9.64 (0.015)[a]	12.9 (0.006)[b]	9.64 (0.005)[b]
M1	—	0.064 (0.004)[c]	1.5	0.046 (0.003)[c]	0.406 (0.005)[d]	0.258 (0.003)[d]
	+ABT	0.032 (0.002)[c]	1.5	0.003 (0.001)[c]	0.031 (0.001)[d]	0.031 (0.001)[d]
M2[e]	—	17.8	1.25	15.8	3.71	3.15
	+ABT	20.3	1.5	11.7	6.73	4.25

—, Not done; AUC, area under the curve.
[a]Unbound concentrations, f^u 0.0016.
[b]Nonspecific binding, $f^u < 0.005$.
[c]Unbound concentrations, f^u 0.06.
[d]Nonspecific binding, f^u 0.011.
[e]Unbound concentrations for M2 not determined.

Downloaded from dmd.aspetjournals.org at ASPET Journals on March 14, 2015

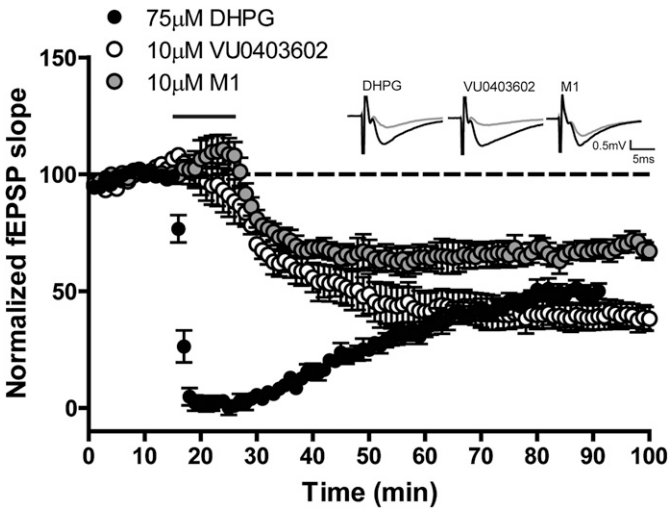

Fig. 6. VU0403602 and M1 (VU0453103) induce long-term depression at the Schaffer collateral-CA1 synapse in hippocampus. A stimulus that produced a 50%–60% fEPSP slope was used as baseline stimulation for each recording. Bath application of 75 μM DHPG for 10 minutes (solid line) induced LTD that lasted at least 55 minutes after washout (n = 8). Similarly, bath application of either 10 μM VU0403602 or 10 μM M1 for 10 minutes (solid line) resulted in LTD that lasted at least 55 minutes after washout of the compound (n = 8, 7, respectively). Insets are sample traces measured predrug (black) or 55 minutes after compound washout (gray). Data represent mean ± S.E.M.

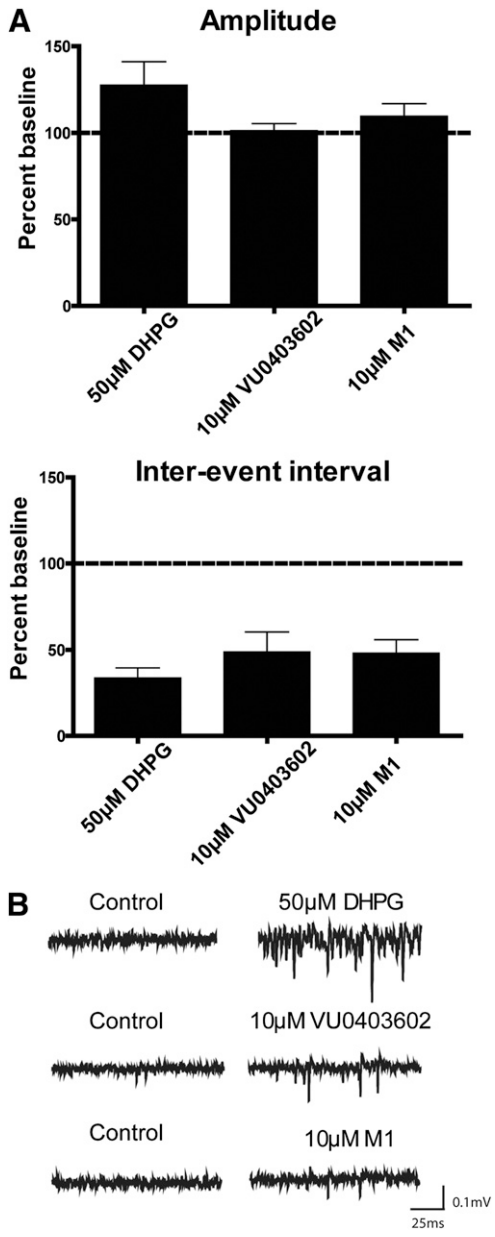

Fig. 7. VU0403602 and M1 (VU0453103) induce epileptiform activity in CA3 neurons in hippocampus. Amplitude and interevent interval of spontaneous firing were determined using field potential recordings in CA3 in the hippocampal formation. (A) Application of 50 μM DHPG (n = 11), 10 μM VU0403602 (n = 8), or 10 μM M1 (n = 7) for 10 minutes resulted in a robust decrease in the interevent interval of spontaneous events while having no significant effect on amplitude of spontaneous events. Data represent mean ± S.E.M. (B) Sample traces from individual experiments taken before and after the addition of the compound.

inducing the pronounced AEs that we observed after the administration of the parent ligand VU0403602. Previously, after VU0403602 administration to rats (i.p., 30 mg/kg), we observed a rapid T_{max} of both the parent ligand VU0403602 (T_{max}, 0.25 hour) and M1 (T_{max}, 0.25 hour), as well as concurrent onset of behavioral AEs that marked this rodent neurotoxicity. After direct administration of M1 to rats (i.p., 30 mg/kg), we observed a similar rapid onset of AEs (Fig. 8). Moreover, the M1-mediated AEs were strikingly similar to those achieved by systemic administration of VU0403602 and the aforementioned ago-PAM, VU0422465, the occurrence of which were characterized by seizures, forelimb asymmetry, tremor, and facial bleeding. Considering the rapid formation of M1 in vivo, its extensive distribution to the CNS, and the consistency between the P450-mediated formation of M1 and the subsequent mitigation of AEs following ABT pretreatment, we submit that this metabolite contributes to the in vivo toxicity observed in rats via an $mGlu_5$ receptor-mediated mechanism.

Discussion

In an effort to advance new approaches in the treatment of the negative and cognitive symptoms common among schizophrenia patients, we have identified PAMs of $mGlu_5$ as potential novel therapeutics to rescue the *N*-methyl-D-aspartate receptor hypofunction believed to underpin this devastating neurologic disorder (Olney et al., 1999; Tsai and Coyle, 2002; Williams et al., 2011; Rook et al., 2012). Herein, we have introduced an $mGlu_5$ PAM, VU0403602, residing within a biarylacetylene scaffold that, in addition to displaying robust potency and a corresponding ninefold shift in the glutamate response, also displayed an intrinsic partial agonist profile in vitro (31.1 nM; 49% Glu_{max}). Such ago-PAMs have previously been shown to produce efficacy in preclinical models of psychosis, such as in the reversal of amphetamine-induced hyperlocomotion rodent model (Noetzel et al., 2012; Rook et al., 2012). Indeed, after i.p. administration of VU0403602 to S-D rats, VU0403602 produced a dose-dependent reversal of hyperlocomotion, with a minimally active dose of 3 mg/kg.

However, similar to previous reports from our laboratories regarding the systemic administration of ago-PAMs to rodents (e.g., VU0422465), we observed an AE profile in rats after systemic administration of VU0403602 characterized by behavioral disturbances such as seizure activity (Noetzel et al., 2012; Rook et al., 2012). The onset of behavioral disturbances was dose- and concentration-dependent, and the severity of the AEs increased with time as measured by Racine scoring methodology. Moreover, the neurotoxicity observed in rats was discovered to be target-mediated, as coadministration of VU0403602 with an allosteric antagonist of $mGlu_5$ (MPEP) effectively blocked the onset of AEs. Interestingly, an in vitro metabolism appraisal implicated oxidative metabolism as the primary biotransformation

Downloaded from dmd.aspetjournals.org at ASPET Journals on March 14, 2015

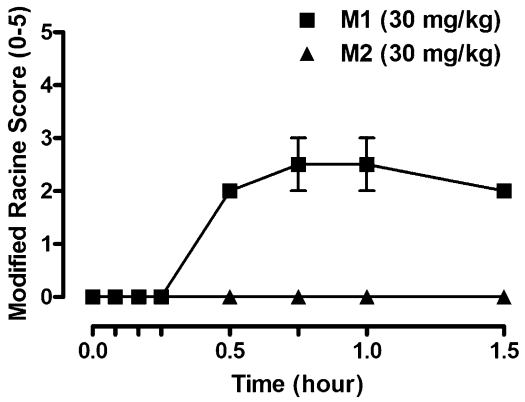

Fig. 8. The $mGlu_5$ ago-PAM metabolite M1 induces dose- and time-dependent increases in behavioral adverse effects in male Sprague-Dawley rats receiving a single administration (i.p., 30 mg/kg, $n = 2$), whereas the inactive metabolite M2 is devoid of AEs (i.p., 30 mg/kg, $n = 2$). Data represent mean ± S.E.M.

pathway for VU0403602, resulting in the formation of a principal hydroxylated metabolite M1 (+16 Da) in Sprague-Dawley rat hepatic subcellular fractions (e.g., S9). Having demonstrated the P450-mediated mechanism of M1 formation in vitro, we examined the extent of P450 metabolism in vivo and determined M1 to be the principal oxidative metabolite detected in the circulation and central nervous system (i.e., brain tissue analysis) of rats receiving VU0403602 (Kalvass and Maurer, 2002; Liu et al., 2008). Moreover, the distribution of M1 to the CNS ($AUC_{0-\infty}$) was discovered to be approximately ~6:1 relative to the plasma of rats receiving VU0403602. Coupled with an unbound brain fraction (f_u) of 0.011 for M1, the CNS distribution of the primary oxidative metabolite (M1) far exceeded that of the parent modulator, VU0403602 ($AUC_{0-\infty}$ brain-to-plasma, ~2:1; brain f_u, < 0.001).

Previously established structure-activity relationships (SAR) for allosteric modulation of $mGlu_5$ indicated a range of tolerance for oxidation (e.g., hydroxylation) of this scaffold with respect to resulting PAM activity of analogs, including switches in primary pharmacology to NAMs and SAMs (Sharma et al., 2009; Lindsley, 2011; Wood et al., 2011). Considering mono hydroxylation of organic molecules is a common outcome of P450–mediated metabolism, we hypothesized a role of DMEs in the AEs observed in vivo following VU0403602 administration to rats. Importantly, rats that were pretreated with the pan P450 inactivator, ABT, failed to manifest the AEs previously demonstrated following VU0403602 exposure, implicating the role of an oxidative metabolite (e.g., M1) in the induction of in vivo neurotoxicity. Indeed, in vitro investigations revealed a pharmacological profile for M1 characterized by a mixed ago-PAM profile in rat $mGlu_5$-expressing cells. Although the PAM efficacy of M1 was similar to VU0403602 (8.2- and 9.0-fold left-shift in glutamate potency, respectively), we noted an agonist profile of higher efficacy for the metabolite (≈80% Glu_{max}) compared with that of VU0403602 ($< 50\%$ Glu_{max}). Likewise, the ago-PAM character of M1 was observed in the electrophysiological assessments, as exposure of rat hippocampal slices to the metabolite alone induced profound LTD at the SC-CA1 synapse, as well as epileptiform activity in area of CA3 of the hippocampus. The present findings are in agreement with previous data from our laboratory and other recent reports demonstrating that direct agonists and mixed ago-PAMs can over activate $mGlu_5$ and perturb normal neuronal activity in rats, which can include an induction of epileptiform activity in distinct hippocampal regions (e.g., CA3) (Lee et al., 2002; Wong et al., 2005; Rook et al., 2012). Although VU0403602 was able to induce LTD and epileptiform activity in vitro, its intrinsic partial agonism and overall lower efficacy in vivo appears insufficient to induce overt adverse effects on its own (i.e., in the presence of the P450 inactivator ABT) and at the concentrations achieved in the present studies. It is also possible that VU0403602 and M1 may have differential effects in varied brain regions that are known to express $mGlu_5$. Ultimately, these findings serve to underscore the importance of avoiding allosteric agonist activity in the design of $mGlu_5$ modulators and thereby retaining dependency on activation of $mGlu_5$ by endogenous glutamate activity for the safe and efficacious modulation of $mGlu_5$.

Recent academic and pharmaceutical research accounts of proconvulsant side effects arising from overactivation of $mGlu_5$ may represent an impediment to the development of $mGlu_5$-targeted allosteric modulators for the treatment of schizophrenia (Rook et al., 2012; Parmentier-Batteur et al., 2013). Recent reports from our laboratory comparing PAMs with ago-PAMs support the hypothesis that positive allosteric modulators of $mGlu_5$ that are devoid of intrinsic agonist activity do not carry proconvulsant and epileptogenic side effect liabilities; however, a recent publication describes an $mGlu_5$ PAM devoid of agonist activity, which nevertheless carried seizure-like adverse effects in rodents (Noetzel et al., 2012; Rook et al., 2012; Parmentier-Batteur et al., 2013). The present report highlights the possibility that in vivo biotransformation of $mGlu_5$ PAMs may result in the CNS exposure of a potent metabolite ligand that bears noticeable switches in pharmacology and/or pharmacokinetic disposition that are distinct from its parent ligand.

Most SAR common to classes of enzyme inhibitors or receptor agonists or antagonists targeting orthosteric sites often display an intolerance with respect to structural modifications that are installed by DMEs (e.g., P450s), resulting in the pharmacological deactivation of the chemotherapeutic agent. The biotransformation of allosteric receptor modulators and/or allosteric enzyme inhibitors/activators by DMEs represents an unexpected hurdle for rational drug design efforts due to the possibility of metabolism-mediated formation of active metabolites, ligands that either display pharmacology distinct from that of the parent compound or bear potent intrinsic agonist activity that exceeds that of the parent compound, as is the apparent case with VU0403602. The SAR observed in allosteric receptor modulation are sensitive to subtle, single atom modifications commonly catalyzed by so-called phase I oxidative enzymes (e.g., P450, flavin monooxygenases, aldehyde oxidase), thus oxidative metabolism could bioactivate a parent compound to a metabolite-ligand, which could attenuate or exacerbate the desired pharmacodynamic effects, seriously complicating proof-of-concept studies and/or the safety assessment of a clinical candidate. These and other related scenarios underline the importance of continued basic science development into understanding the biotransformation and metabolic fate of allosteric modulators for the potential treatment of human disease.

Downloaded from dmd.aspetjournals.org at ASPET Journals on March 14, 2015

Authorship Contributions

Participated in research design: Bridges, Rook, Noetzel, Morrison, Jones, Niswender, Xiang, Stauffer, Conn, Daniels.

Conducted experiments: Bridges, Rook, Noetzel, Morrison, Vinson.

Contributed new reagents or analytic tools: Zhou, Gogliotti, Lindsley, Stauffer.

Performed data analysis: Bridges, Rook, Morrison, Noetzel, Xiang, Niswender, Daniels.

Wrote or contributed to the writing of the manuscript: Bridges, Rook, Noetzel, Niswender, Lindsley, Stauffer, Conn, Daniels.

References

Balani SK, Miwa GT, Gan LS, Wu JT, and Lee FW (2005) Strategy of utilizing in vitro and in vivo ADME tools for lead optimization and drug candidate selection. *Curr Top Med Chem* **5**: 1033–1038.

Balani SKZ, Zhu T, Yang TJ, Liu Z, He B, and Lee FW (2002) Effective dosing regimen of 1-aminobenzotriazole for inhibition of antipyrine clearance in rats, dogs, and monkeys. *Drug Metab Dispos* **30**:1059–1062.

Conn PJ, Lindsley CW, and Jones CK (2009) Activation of metabotropic glutamate receptors as a novel approach for the treatment of schizophrenia. *Trends Pharmacol Sci* **30**:25–31.

Cosford ND, Roppe J, Tehrani L, Schweiger EJ, Seiders TJ, Chaudary A, Rao S, and Varney MA (2003) [3H]-methoxymethyl-MTEP and [3H]-methoxy-PEPy: potent and selective radioligands for the metabotropic glutamate subtype 5 (mGlu5) receptor. *Bioorg Med Chem Lett* **13**: 351–354.

Gregory KJ, Dong EN, Meiler J, and Conn PJ (2011) Allosteric modulation of metabotropic glutamate receptors: structural insights and therapeutic potential. *Neuropharmacology* **60**: 66–81.

Gregory KJ, Nguyen ED, Reiff SD, Squire EF, Stauffer SR, Lindsley CW, Meiler J, and Conn PJ (2013) Probing the metabotropic glutamate receptor 5 (mGlu5) positive allosteric modulator (PAM) binding pocket: discovery of point mutations that engender a "molecular switch" in PAM pharmacology. *Mol Pharmacol* **83**:991–1006.

Hammond AS, Rodriguez AL, Townsend SD, Niswender CM, Gregory KJ, Lindsley CW, and Conn PJ (2010) Discovery of a novel chemical class of mGlu(5) allosteric ligands with distinct modes of pharmacology. *ACS Chem Neurosci* **1**:702–716.

Kalvass JC and Maurer TS (2002) Influence of nonspecific brain and plasma binding on CNS exposure: implications for rational drug discovery. *Biopharm Drug Dispos* **23**:327–338.

Lamb JP, Engers DW, Niswender CM, Rodriguez AL, Venable DF, Conn PJ, and Lindsley CW (2011) Discovery of molecular switches within the ADX-47273 mGlu5 PAM scaffold that modulate modes of pharmacology to afford potent mGlu5 NAMs, PAMs and partial antagonists. *Bioorg Med Chem Lett* **21**:2711–2714.

Lee AC, Wong RK, Chuang SC, Shin HS, and Bianchi R (2002) Role of synaptic metabotropic glutamate receptors in epileptiform discharges in hippocampal slices. *J Neurophysiol* **88**: 1625–1633.

Lindsley CW (2011) Molecular switches' on mGluR allosteric ligands that modulate modes of pharmacology and/or subtype selectivity, in *7th International Metabotropic Glutamate Receptors Meeting*, Taormina, Italy. *Curr Neuropharmacol* **9(1)**:36

Liu X, Chen C, and Smith BJ (2008) Progress in brain penetration evaluation in drug discovery and development. *J Pharmacol Exp Ther* **325**:349–356.

Marek GJ, Behl B, Bespalov AY, Gross G, Lee Y, and Schoemaker H (2010) Glutamatergic (N-methyl-D-aspartate receptor) hypofrontality in schizophrenia: too little juice or a miswired brain? *Mol Pharmacol* **77**:317–326.

Niswender CM, Johnson KA, Weaver CD, Jones CK, Xiang Z, Luo Q, Rodriguez AL, Marlo JE, de Paulis T, and Thompson AD, et al. (2008) Discovery, characterization, and antiparkinsonian effect of novel positive allosteric modulators of metabotropic glutamate receptor 4. *Mol Pharmacol* **74**:1345–1358.

Noetzel MJ, Rook JM, Vinson PN, Cho HP, Days E, Zhou Y, Rodriguez AL, Lavreysen H, Stauffer SR, and Niswender CM, et al. (2012) Functional impact of allosteric agonist activity of selective positive allosteric modulators of metabotropic glutamate receptor subtype 5 in regulating central nervous system function. *Mol Pharmacol* **81**:120–133.

Obach RS and Reed-Hagen AE (2002) Measurement of Michaelis constants for cytochrome P450-mediated biotransformation reactions using a substrate depletion approach. *Drug Metab Dispos* **30**:831–837.

Olney JW, Newcomer JW, and Farber NB (1999) NMDA receptor hypofunction model of schizophrenia. *J Psychiatr Res* **33**:523–533.

Parmentier-Batteur S, Hutson PH, Menzel K, Uslaner JM, Mattson BA, O'Brien JA, Magliaro BC, Forest T, Stump CA, and Tynebor RM, et al. (2013) Mechanism based neurotoxicity of mGlu5 positive allosteric modulators: development challenges for a promising novel antipsychotic target. *Neuropharmacology*, in press.

Rodriguez AL, Grier MD, Jones CK, Herman EJ, Kane AS, Smith RL, Williams R, Zhou Y, Marlo JE, and Days EL, et al. (2010) Discovery of novel allosteric modulators of metabotropic glutamate receptor subtype 5 reveals chemical and functional diversity and in vivo activity in rat behavioral models of anxiolytic and antipsychotic activity. *Mol Pharmacol* **78**: 1105–1123.

Rook JM, Noetzel MJ, Pouliot WA, Bridges TM, Vinson PN, Cho HP, Zhou Y, Gogliotti RD, Manka JT, Gregory KJ, et al. (2012) Unique signaling profiles of positive allosteric modulators of metabotropic glutamate receptor subtype 5 determine differences in in vivo activity. *Biological Psychiatry* **73(6)**:501–9.

Sharma S, Kedrowski J, Rook JM, Smith RL, Jones CK, Rodriguez AL, Conn PJ, and Lindsley CW (2009) Discovery of molecular switches that modulate modes of metabotropic glutamate receptor subtype 5 (mGlu5) pharmacology in vitro and in vivo within a series of functionalized, regioisomeric 2- and 5-(phenylethynyl)pyrimidines. *J Med Chem* **52**:4103–4106.

Tizzano JP, Griffey KI, and Schoepp DD (1995a) Induction or protection of limbic seizures in mice by mGluR subtype selective agonists. *Neuropharmacology* **34**:1063–1067.

Tizzano JP, Griffey KI, and Schoepp DD (1995b) Receptor subtypes linked to metabotropic glutamate receptor agonist-mediated limbic seizures in mice. *Ann N Y Acad Sci* **765**:230–235, discussion 248.

Tsai G and Coyle JT (2002) Glutamatergic mechanisms in schizophrenia. *Annu Rev Pharmacol Toxicol* **42**:165–179.

Vinson PN and Conn PJ (2012) Metabotropic glutamate receptors as therapeutic targets for schizophrenia. *Neuropharmacology* **62**:1461–1472.

Williams R, Manka JT, Rodriguez AL, Vinson PN, Niswender CM, Weaver CD, Jones CK, Conn PJ, Lindsley CW, and Stauffer SR (2011) Synthesis and SAR of centrally active mGlu5 positive allosteric modulators based on an aryl acetylenic bicyclic lactam scaffold. *Bioorg Med Chem Lett* **21**:1350–1353.

Wong RK, Bianchi R, Chuang SC, and Merlin LR (2005) Group I mGluR-induced epileptogenesis: distinct and overlapping roles of mGluR1 and mGluR5 and implications for antiepileptic drug design. *Epilepsy Curr* **5**:63–68.

Wood MR, Hopkins CR, Brogan JT, Conn PJ, and Lindsley CW (2011) "Molecular switches" on mGluR allosteric ligands that modulate modes of pharmacology. *Biochemistry* **50**: 2403–2410.

Zhao W, Bianchi R, Wang M, and Wong RK (2004) Extracellular signal-regulated kinase 1/2 is required for the induction of group I metabotropic glutamate receptor-mediated epileptiform discharges. *J Neurosci* **24**:76–84.

Address correspondence to: Dr. J. Scott Daniels, Department of Pharmacology, Vanderbilt Center for Neuroscience Drug Discovery, Vanderbilt University Medical Center, Nashville, TN 37232-6600. E-mail: scott.daniels@vanderbilt.edu.

Downloaded from dmd.aspetjournals.org at ASPET Journals on March 14, 2015